PROGRESS IN ION BEAM POWER COUPLING AND ION-DRIVEN HOHLRAUMS ON PBFA II

A.B. Filuk, T.A. Mehlhorn, R.G. Adams, G.O. Allshouse, J.H. Aubert, L.D. Bacon, J.E. Bailey, D.D. Bloomquist, J. Boyes, G.A. Chandler, R.S. Coats, D.L. Cook, J.T. Crow, M.E. Cuneo, M.S. Derzon, M.P. Desjarlais, R.J. Dukart, D.L. Fehl, R.A. Gerber, T.A. Haill, D.L. Hanson, D.R. Humphreys, H.C. Ives, D.J. Johnson, M.L. Kiefer, R.J. Leeper, R.W. Lemke, T.R. Lockner, J.E. Maenchen, M.K. Matzen, M.G. Mazarakis, D.H. McDaniel, E.J. McGuire, C.W. Mendel Jr., P.R. Menge, L.P. Mix, A.R. Moats, T.J. Nash, C.L. Olson, R.E. Olson, T.D. Pointon, J.L. Porter, J.W. Poukey, J.P. Quintenz, T.J. Renk, G.E. Rochau, S.E. Rosenthal, D.C. Rovang, C.L. Ruiz, D.B. Seidel, I.R. Shokair, S.A. Slutz, D.L. Smith, R.W. Stinnett, W.A. Stygar, M.A. Sweeney, and G.C. Tisone

Sandia National Laboratories, Albuquerque, New Mexico, USA

Light ions could provide an efficient driver for high-yield and energy applications of inertial confinement fusion. Working toward this goal, we have demonstrated well-diagnosed, ion-driven hohlraum targets at ~60 eV radiation temperature on the PBFA II accelerator, with specific power deposition of 800-1400 TW/gm. This parameter regime is of interest to both light- and heavy-ion drivers, and corresponds to the early phase of a high-yield target drive. Further increases in target temperature require increasing the ion beam driver intensity. Direct measurements of ion diode dynamics are providing insights to improve our driver capability. Maximum beam intensity is obtained by both increasing the coupled lithium beam power and decreasing the beam microdivergence. The microdivergence of the beam near the ion source appears to be a major contributor early in the beam pulse. Experiments have shown that a parasitic non-lithium ion beam consumes a large fraction of the available power. Calculations indicate the coupled beam power can be increased by up to a factor of 3 by eliminating this parasitic loss. Preliminary experiments to clean the ion diode surfaces are under way.

1. Introduction

Light ions are being studied as an efficient driver for Inertial Confinement Fusion (ICF) high yield and energy applications. The long-term goals of the light-ion ICF program at Sandia National Laboratories (SNL) are to demonstrate light-ion-driven ICF fusion yields in the 200-1000 MJ range in a Laboratory Microfusion Facility (LMF) [1], and to determine if light ions are the best driver for longer-term ICF energy applications [2]. Light-ion ICF uses pulsed-power compression techniques and magnetically-insulated transmission lines (MITLs) to transform microsecond-scale electrical power to a 20-50 ns pulse of 10^{14}-10^{15} W power. This power is fed to an applied-B ion diode to generate an intense ion beam pulse; the diode uses strong applied magnetic fields to insulate electron flow across the diode anode-cathode (AK) gap while allowing the more-massive ions to be accelerated across the AK gap. The accelerated ion beam is transported to a hohlraum target, typically using a gas transport region for charge and current neutralization in order to maintain the beam's focusability. The foam-filled hohlraum target at the beam focus converts the ion beam power to x-ray radiation power. A fuel capsule in the hohlraum would be driven by the radiation pulse to generate fusion energy in the usual indirect-drive ICF scheme [3]. Thus light-ion ICF involves the conversion of pulsed-power to ion beam power in an ion diode, transport of the ion beam, and the subsequent conversion of ion beam power to radiation power in a hohlraum. This paper will discuss progress in both electrical-to-beam power conversion and beam-to-radiation power conversion. Transport experiments are being done at SNL and other col-

laborating facilities, but will not be discussed here. The critical issue presently is generation of a sufficiently-intense ion beam.

Our long-term goal of high-yield ICF places requirements on the capsule/hohlraum design, which in turn sets the requirements for the light-ion driver. A detailed study for an LMF-scale design used 2- and 3-dimensional ion deposition and radiation transport codes, and a 2-dimensional radiation-hydrodynamics code to give requirements for beam symmetry, energy, intensity, and stand-off (transport) of the ion driver [1]. A two-phase drive pulse would be used (see Figure 1) with 12 beams in each pulse phase illuminating a spherical hohlraum to provide the necessary symmetry. The first phase, the foot

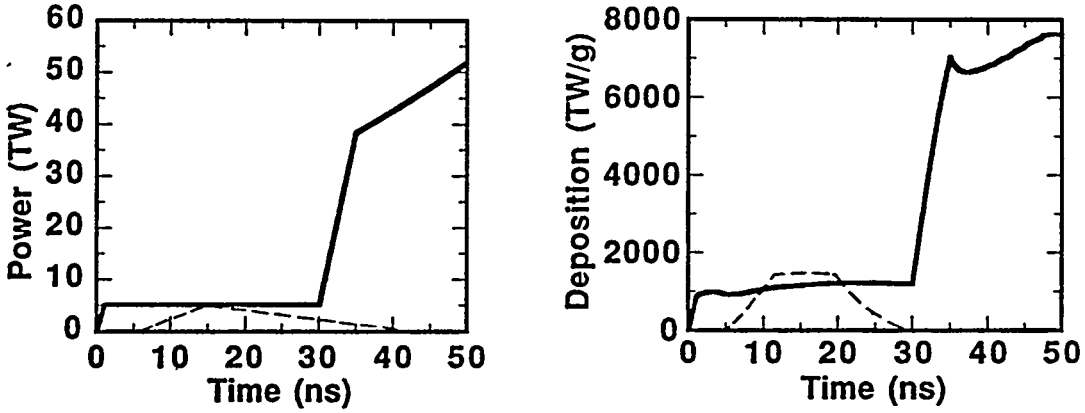

FIGURE 1. Ion beam power at target and specific power deposition for each module of a 12-module LMF high-yield design. The dashed lines indicate present performance of PBFA II.

pulse, would use ~5 TW/cm^2, 17-24 MeV, 30 ns lithium ion beams with a specific power deposition of ~1000 TW/gm in the hohlraum foam to heat the hohlraum to radiation temperatures close to 100 eV. The second phase, the main pulse, would use ~50 TW/cm^2, 28-35 MeV ramped-energy lithium beams to heat the hohlraum to ~250 eV and drive the capsule to ignition and ICF burn. The total peak beam power at the target would be about 700 TW. Internal-pulse-shaping layers on the capsule would tailor the radiation drive to maximize efficiency of the two-phase drive pulse [4]. The design analysis indicates a fusion yield in excess of 500 MJ for this type of target.

2. Progress in Ion-Driven Hohlraums

At present we are studying ion driver and target physics issues on the Particle Beam Fusion Accelerator II (PBFA II). This device provides lithium ion beam power and specific power deposition in a regime comparable to that of the LMF-scale foot pulse (see Figure 1). The central diode region of the large device is shown in Figure 2. A radially-converging ion beam illuminates a cylindrically-symmetric foam-filled hohlraum target of about 8 mm diameter. The same principles are used in extraction geometry ion diodes, such as on the SABRE accelerator at SNL and those anticipated for the LMF, in order to obtain an annular ion beam that can be propagated away from the diode vicinity. Using our present 9 MeV, 7-9 TW, ~1.5 TW/cm^2 lithium ion beam we achieve specific power depositions of 800-1400 TW/gm, in a regime of interest to both light- and heavy-ion-driven ICF. Figure 3 shows a plot adapted from one by Bock [5], illustrating the parameter regimes achieved in PBFA II hohlraum experiments. Key target physics issues are ion energy deposition in the foam and radiation conversion, radiation symmetrization, and internal pulse shaping of the radiation drive at the capsule.

Our first targets were driven by protons. These well-diagnosed [6], proof-of-principle experiments in cylindrical hohlraums demonstrated the first ion-driven hohlraums, achieving 35 eV radiation tem-

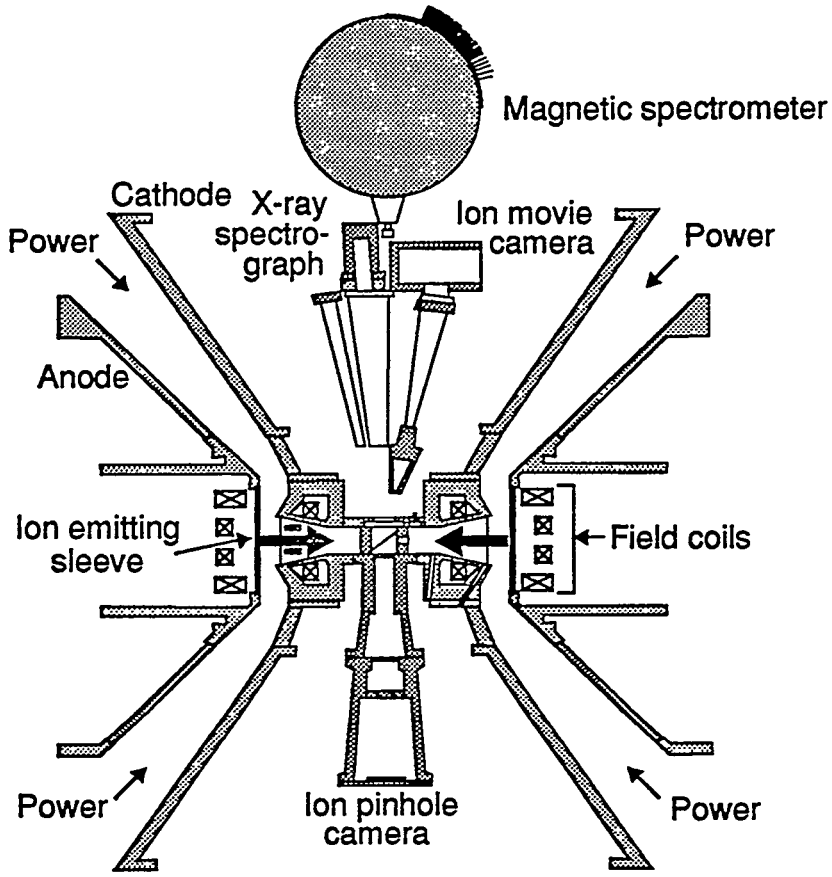

FIGURE 2. Schematic of central section of PBFA II, showing conical power feeds, ion-emitting source, and radially-directed ion beam (thick arrows). On a target experiment the thin 45° Rutherford-scattering foil at the center is replaced by a hohlraum target. Some of the beam diagnostics are indicated.

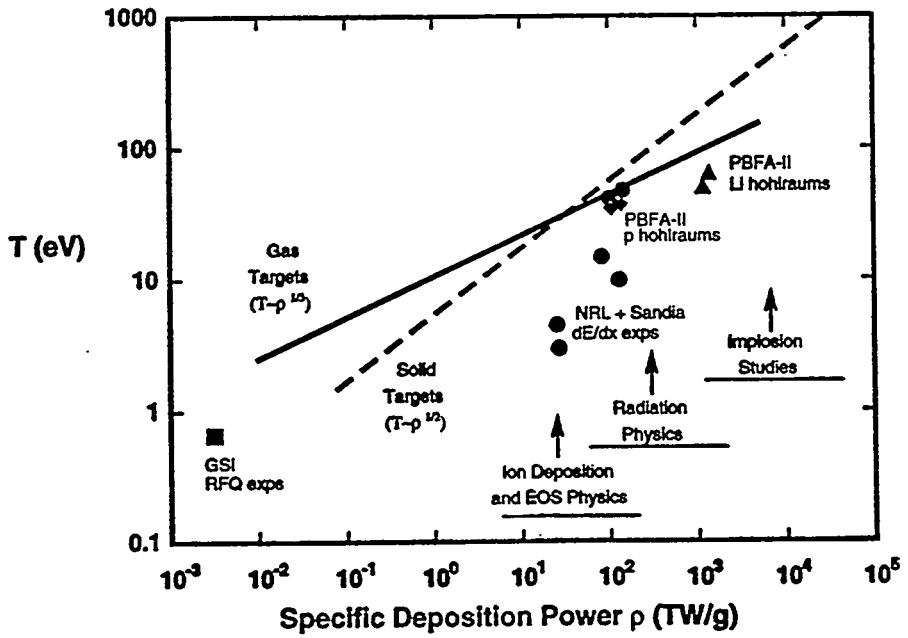

FIGURE 3. Target radiation temperature T_R vs. specific power deposition ρ for ion-driven targets, from original figure by Bock [5]. Parameters achieved in target experiments on PBFA II are indicated.

perature at specific power deposition of 120 TW/gm [7][8]. The long stopping range of protons in the target material meant these targets were not matched to the driver beam. Achieving significantly higher target temperatures using protons as a driver ion would require extremely large currents, a high-risk strategy for ion diode operation and beam transport. Instead, a non-protonic light ion with shorter range can provide more efficient heating in a hohlraum still large enough to permit radiation symmetrization. Li^+ was selected because its high ionization potential allows maximum charge state selectivity in the diode ion source, and its optimal range in a target can be achieved with our pulsed-power voltages.

Our first lithium-driven hohlraum experiments used an open conical shape to facilitate viewing the interior of the ~1 cm diameter, foam-filled, gold wall hohlraum (Figure 4). The comprehensive diag-

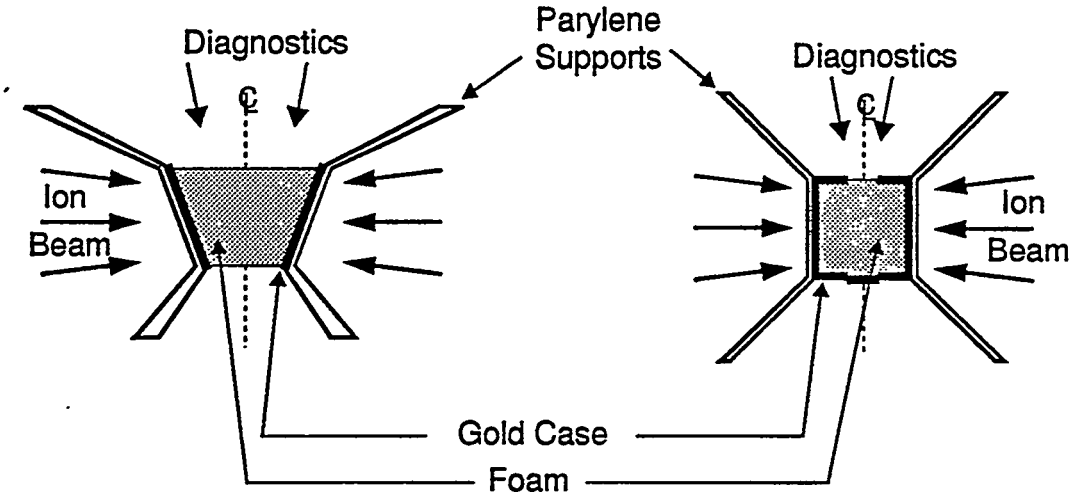

FIGURE 4. Schematic cross-section of the two types of lithium-driven hohlraums used on PBFA II. No fusion capsule was present.

nostic suite [9] yielded a number of key results that agree well with 1- and 2-dimensional radiation hydrodynamic calculations [4]. Filtered x-ray diode detector and bolometer arrays showed a broad-band spectrum consistent with Planckian emission and indicated a radiation temperature of 58±6 eV. Space- and time-resolved grazing incidence and transmission grating spectrometers yielded detailed spectra. Time-integrated and time-resolved x-ray pinhole cameras and 1-dimension streaked x-ray imaging showed features of the gold radiation case wall viewed through the foam, demonstrating that the foam became optically thin to the x-rays and that the foam tamped expansion of the hohlraum wall.

Recent lithium-driven hohlraum experiments used a more closed, cylindrical hohlraum to improve the radiation containment and to test diagnosis through small holes in the radiation case (Figure 4). The target diagnostics listed above viewed a 1.5 mm or 3 mm diameter hole in the top of the hohlraum, while a shock-breakout diagnostic was used on the bottom of the hohlraum [10]. The latter diagnostic uses a laser to monitor the time-dependent change in reflectivity of a 2-step thin Al cover on the bottom hole of the hohlraum. The reflectivity change is caused by the arrival of the ablation-driven shock at the outer surfaces, and allows the radiation drive to be characterized. Analysis of these hohlraum data are still in progress.

We have demonstrated well-diagnosed, ion-driven hohlraums. Key target physics issues of ion energy deposition, radiation conversion, and radiation symmetrization have been addressed experimentally and modelled with our capabilities. No anomalous results have been observed so far; hohlraum heating by ion beams appears to work as expected. Higher temperature hohlraums require greater beam intensity on target; the present lithium focal intensity of ~1.5 TW/cm^2 will have to be increased by a factor of 3-4 to achieve our near-future goal of 100 eV hohlraums.

3. Progress in Ion Beam Power Coupling

The lithium beam parameters listed in Table 1 summarize our present capability, our near-term goal for 100 eV hohlraums, and what would be needed for each of the 12 main-pulse modules of an LMF-scale high-yield device [1]. Note that if one assumes a constant ion source emittance then a 22 mrad

TABLE 1. Lithium driver beam parameters at present and those required to meet near-term goal and LMF high-yield. Focal intensity is averaged over a 6 mm diameter sphere. In LMF design beam power at target will double because of beam bunching.

Parameter	Present	Near-future	LMF module
Ion Energy (MeV)	9	9	28-35
Focal Intensity (TW/cm^2)	1.5	5-6	~50
Beam Power (TW)	6-8	15-22	27
Microdivergence (mrad)	22-25	16-22	6
Hohlraum Temperature (eV)	~60	~100	~250

beam microdivergence (half-angle beam spread) at 9 MeV corresponds to a 12 mrad microdivergence at 30 MeV, so that the microdivergence needs to be improved by a factor of about 2 to satisfy our LMF requirement. Increased beam intensity is critical to meeting our near-term goal. For an ideal, 2-dimensional Gaussian beam intensity profile, the focussed ion beam intensity on target is proportional to the power coupled into the beam and inversely proportional to the square of the beam microdivergence. The actual coupled beam power and beam microdivergence limits depend on detailed MITL and diode physics. Figure 5 shows calculated beam intensity as a function of beam power in the diode for various beam microdivergences, assuming 70% of the beam power is available at the focus. The most effective way to both increase beam intensity and establish a clear path to the LMF parameters of Table 1 is to

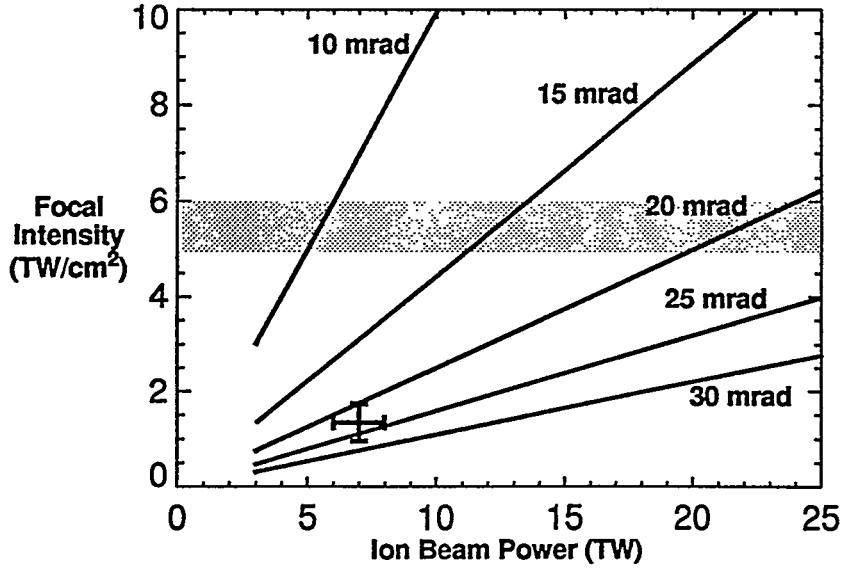

FIGURE 5. Ion beam focal intensity (averaged over a 6 mm spherical focus) as a function of beam power in the diode for various beam microdivergence values. Present PBFA II parameter regime is indicated by crossed bars. Shaded region shows parameter range required for near-term goal.

maximize coupled beam power and minimize beam microdivergence. We are making progress on both of these issues.

To improve diode performance, we are studying diode physics in unprecedented detail. Much can be learned from careful measurements of the beam during transport and at the focus by using a variety of Rutherford-scattering particle diagnostics as shown in Figure 2 [11]. Other diagnostics such as filtered Faraday cups and multiple dB/dt loops just outside the diode AK gap provide data on our parasitic losses (see below). However, it is difficult to probe the AK gap dynamics directly and non-invasively. Spectroscopy of neutral emissions in the AK gap is providing a detailed picture of ion and electron charge dynamics. These time- and 1-dimensional space-resolved observations of the Stark shift of optical emission from the ~10 MV/cm electric fields in the AK gap yield unfolded snapshots of the diode charge distribution, showing the growth of electron density across the gap as the ion current rises. The measurements are directly compared with results from the powerful, 3-dimensional, fully electromagnetic particle-in-cell (PIC) code QUICKSILVER [12] to check our understanding of ideal diode behavior and to assess the role of non-ideal effects [13]. One significant observation is that the LiF-coated anode ion source has a high electric field at the surface rather than the zero field expected for a space-charge-limited source. We are incorporating these results into our analytic diode equilibrium model [14] and our QUICKSILVER numerical model. The goal of these types of measurements is to understand and then modify the detailed physics that determines performance limits of actual ion diodes.

Improved beam microdivergence requires measuring and understanding the growth in microdivergence from the ion source to the beam focus on target. There are many possible contributions to the final beam microdivergence, including the ion source, non-uniform emission effects, instabilities in the diode AK gap, varying canonical angular momentum at the gas transport cell charge-stripping window, and micro-charge clumping instability [15] in quasi-charge-neutralizing regions. Both ion movie camera and magnetic spectrometer measurements indicate 22-25 mrad beam microdivergence at the beam focus. Near-anode AK gap spectroscopy of Doppler-broadened emission is used to infer the microdivergence at the LiF ion source; typically 14-20 mrad of the final microdivergence appears to be due to the ion source. Figure 6 shows unfolded time-dependent beam microdivergence histories measured at the beam focus and inferred spectroscopically from the ion source, along with the beam power. Note that early in the pulse the microdivergence at the focus seems to be dominated by the source contribution, while a growing non-source component rises steadily. We are continuing to assess the present field-emission Li^+ ion source behavior while also developing and characterizing other plasma-type Li^+ ion sources [16]. The growing non-source microdivergence may be caused by a growth and frequency shift of instabilities in the diode AK gap. The strong velocity shear of the E×B azimuthally-drifting electron sheath in the AK gap drives strong fluctuations; the resulting clumped electron charge in the AK gap can deflect the beam ions if the period of the fluctuations is comparable to the ion gap-crossing time, giving rise to an instability-induced microdivergence. We have studied this phenomenon both analytically [17][18] and numerically with QUICKSILVER [18][19]; indications of the predicted energy and canonical angular momentum correlation at the phase velocity of the instability have been seen in the magnetic spectrometer diagnostic. The simulations predicted a lower divergence when the sheath was kept further away from the anode (giving lower ion beam current), an effect that has been seen in experiments elsewhere [20][21]. Another technique we have demonstrated for lower beam microdivergence is the use of two-stage diodes, where the first stage operates at lower voltage to establish the beam current while the second stage accelerates this beam to full energy and reduces the angular velocity spread [22][23]. Understanding and reducing the overall beam microdivergence is critical to meeting our long-term LMF design requirements.

We have significantly improved our understanding of the coupled ion beam power [24]. Measurements and circuit modeling show that approximately 35 TW of pulsed electrical power is available at the start of our vacuum MITLs, but only about 7-9 TW of that power is actually coupled into the lith-

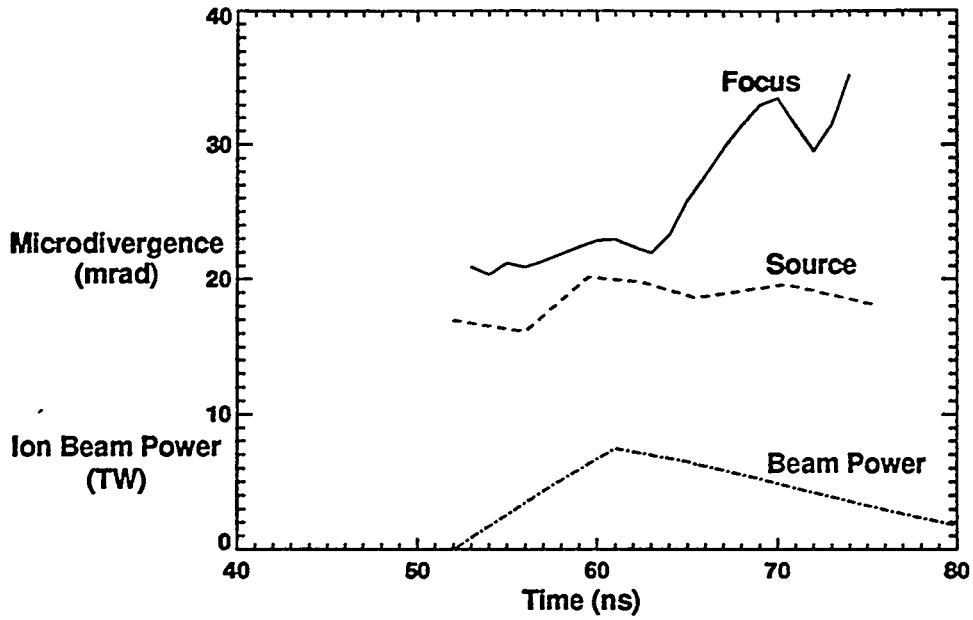

FIGURE 6. Time-dependent beam microdivergence at the beam focus and that due to the ion source, along with beam power at the diode. Note the large microdivergence contribution from the ion source.

ium beam. A large parasitic loss in the diode vicinity consumes about two-thirds of our potential lithium beam power. We have used extensive MITL circuit analysis and the 2-dimensional electromagnetic PIC code TWOQUICK [12] to show that the voltage-adder-launched electron flow along the MITLs does not couple efficiently to the higher-impedance ion diode, resulting in a substantial energy loss outside the diode region from the electron losses to the anode. Detailed dB/dt, filtered Faraday cup, nuclear activation, magnetic spectrometer, and Thomson parabola measurements give an accounting for the energy losses from the near-diode MITL feed region down to and including the ion beam. These results show that about 32% of the 530 kJ of energy delivered to the MITLs near the ion diode is given up in electron losses to the anode and near-diode power feed. The remaining 68% of the energy goes into ion beam generation; typically 38% of this beam energy goes into lithium ions, 25% goes into carbon, oxygen, and fluorine ions, and 37% goes into protons. The parasitic power loss is going into these non-lithium beam ions that are predominantly contaminants on the anode surface. Our diode is driving lithium and non-lithium beams in parallel, with the non-lithium beam dominating the current later in the pulse. A diode/MITL modelling calculation with an anode that has both field-emission Li^+ regions and space-charge-emission H^+/C^+ regions shows good agreement with observed diode impedance behavior. Eliminating the parasitic loss in the model indicates that the peak lithium beam power could be increased by up to a factor of 3, as shown in Figure 7.

We are using vacuum surface cleaning techniques in the diode region in an attempt to eliminate this parasitic loss current and significantly increase our beam current. The problem of desorbed surface impurities affecting a plasma device's performance is familiar to the tokamak community, where large improvements in performance were obtained by cleaning and conditioning the vacuum vessels. We are testing cleaning methods on the smaller SABRE extraction ion diode and will transfer the technology and optimum cleaning techniques over to PBFA II this year. The SABRE diode uses the same ion source as on PBFA II, at about 1/5 the lithium current density. The present cleaning approach is to use Ar and Ar/O_2 gas mixtures in an RF discharge for periods of about an hour in order to physically or chemically sputter impurities from the anode surface. We use continuous vacuum pumping to remove the desorbed impurities during the discharge period. The anode surface is heated to 500°C to outgas impurities and reduce the re-sticking probability of the desorbed impurity atoms. The discharge is ter-

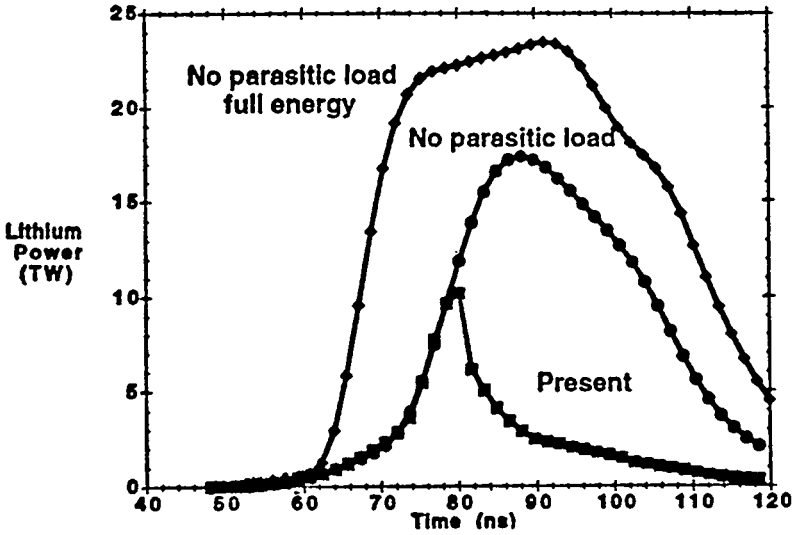

FIGURE 7. Model calculation of lithium beam power history with and without parasitic loss, operating PBFA II at 3/4 energy (present), and at full energy.

minated and the machine is pumped down immediately prior to the shot. SABRE results to date have shown that the lithium beam current density and total lithium content are approximately doubled when cleaning techniques are used. Similar improvements on PBFA II at higher power levels are anticipated and are being tested presently. It is possible that any microdivergence caused by non-uniform ion emission at the anode may also be improved as the anode surface is cleaned of impurities, however no significant change in beam microdivergence has been seen in SABRE cleaning experiments.

Eliminating the non-lithium parasitic loss current and reducing the beam microdivergence modestly will allow us to reach our near-term goal and continue to study ion-driven hohlraum physics issues. More importantly, the basic diode physics understanding accompanying the parameter improvements should establish a high degree of confidence in scaling of our results to full LMF parameters.

Acknowledgments

Yitzhak Maron of the Weizmann Institute has provided valuable insights and suggestions on diode physics. Dale Welch of Mission Research Corporation modelled the effect of parasitic ion beams arising from neutral ionization in the diode. Collaborating laboratories worldwide contribute to the progress in light-ion drivers, and we are particularly grateful to those at Cornell University, ILE Osaka University, Kernforschungszentrum Karlsruhe, Naval Research Laboratories, Weizmann Institute, and University of Wisconsin. This work would not be possible without the efforts of many diagnostic technicians, SNL support staff, and the PBFA II operations team. Funding was provided by the U.S. Department of Energy under contract DE-AC04-94-AL85000.

DISCLAIMER

References

1. OLSON, R.E., et al, "The Light Ion LMF and Its Relevance to IFE", in *Proceedings of the 15th IEEE-NPSS Symposium on Fusion Engineering, October 11-15, 1993, Hyannis, Massachusetts*, p. 189.
2. OLSON, R.E., et al, "The Light Ion Beam Approach to ICF Energy Production", in *Proceedings of the American Nuclear Society 11th Topical Meeting on the Technology of Fusion Energy, June 19-23, 1994, New Orleans, Louisiana.*
3. See, for example, *Nuclear Fusion by Inertial Confinement*, eds. G. Velarde, Y. Ronen, J.M. Martinez-Val (CRC Press, Ann Arbor, 1993).
4. MATZEN, M.K., et al, "Progress in Ion Beam Target Design and Experiments", in *Proceedings of the 15th International Conference on Plasma Physics and Controlled Nuclear Fusion Research, Sept. 26-Oct. 1, 1994, Seville, Spain.*
5. BOCK., R., "Status and Perspectives of Heavy Ion Inertial Fusion", GSI-91-13 report (1991).
6. CHANDLER, G.A., et al, Rev. Sci. Instr. 63,4828 (1992).
7. DERZON, M., et al, Rev. Sci. Instr. 63, 5068 (1992).
8. COOK, D.L., et al, Plasma Physics and Controlled Nuclear Fusion Research 3, 63 (1992).
9. LEEPER, R.J., et al, "Target Diagnostics for Intense Lithium Ion Hohlraum Experiments on PBFA II", submitted to Rev. Sci. Instr.
10. LUDMIRSKY, A., et al, J. Phys. E: Sci. Instr. 19, 309 (1986).
11. LEEPER, R.J., et al, Rev. Sci. Instr. 59, 1860 (1988).
12. QUINTENZ, J.P., et al, Laser & Particle Beams, 12, 283 (1994).
13. BAILEY, J.E., et al, "Measurements of Acceleration Gap Dynamics in a 20 TW Applied-B Ion Diode", submitted to Physical Review Letters.
14. DESJARLAIS, M.P., Phys. Fluids B 1, 1709 (1989).
15. OLSON, C.L. and POUKEY, J.W., "Divergence in Intense Ion Beams Caused By Incomplete Charge Neutralization", in *Proceedings of the 9th International Conference on High-Power Particle Beams, May 25-29, 1992, Washington, D.C.*, p. 897.
16. RENK, T.J., et al, "LEVIS Ion Source and Beam Characterization on PBFA II", in *Proceedings of the 10th International Conference on High-Power Particle Beams, June 20-24, 1994, San Diego, California*, to be published.
17. LEMKE, R.W. and SLUTZ, S.A., "A full mode set electromagnetic stability analysis of magnetically insulated ion diodes", to be published in Physics of Plasmas.
18. DESJARLAIS, M.P., et al, Phys. Rev. Lett. 67, 3094 (1991).
19. POINTON, T.D., et al, Phys. Plasmas 1, 429 (1994).
20. BLUHM, H., et al, "Focussing Properties of a Strongly Insulated Applied-B_r Proton Diode with a Preformed Anode Plasma Source", in *Proceedings of the 9th International Conference on High-Power Particle Beams, May 25-29, 1992, Washington, D.C.*, p. 51.
21. GREENLY, J.B., et al, in *Proceedings of the 10th International Conference on High-Power Particle Beams, June 20-24, 1994, San Diego, California*, to be published.
22. LOCKNER, T., et al, "Theoretical and Experimental Studies of the 2-Stage Ion Diode", in *Proceedings of the 1993 IEEE Pulsed Power Conference, Albuquerque, New Mexico.*
23. SLUTZ, S.A., et al, Phys. Plasmas 1, 2072 (1994).
24. MEHLHORN, T.A., et al, "Progress in Lithium Beam Power, Divergence, and Intensity at Sandia National Laboratories", in *Proceedings of the 10th International Conference on High-Power Particle Beams, June 20-24, 1994, San Diego, California*, to be published.